

**“Secular and Rotational Light Curves
of 6478 Gault”**

Ignacio Ferrín
Institute of Physics, FACOM and SEAP, University of Antioquia,
Medellín, Colombia, 05001000
ignacio.ferrin@udea.edu.co

Cesar Fornari
Observatorio “Galileo Galilei”, X31
Oro Verde, Argentina

Agustín Acosta
Observatorio “Costa Teguisse”, Z39
Lanzarote, España

Number of pages 22

Number of Figures 11

Number of Tables 5

Abstract

We obtained 877 images of active asteroid 6478 Gault on 41 nights from January 10th to June 8th, 2019, using telescopes. We created the phase, secular and rotational light curves of Gault, from which several physical parameters can be derived. From the phase plot we find that no phase effect was evident. This implies that an optically thick cloud of dust surrounded the nucleus hiding the surface. The secular light curve (SLC) shows several zones of activity the origin of which is speculative. From the SLC plots a robust absolute magnitude can be derived and we find $m_V(1,1,\alpha) = 16.11 \pm 0.05$. We also found a rotational period $P_{rot} = 3.360 \pm 0.005$ h and show evidence that 6478 might be double. The parameters of the pair are derived. Previous works have concluded that 6478 is in a state of rotational disruption and the above rotational period supports this result. Our conclusion is that 6478 Gault is a suffocated comet getting rid of its suffocation by expelling surface dust into space using the centrifugal force. This is an evolutionary stage in the lifetime of some comets. Besides being a MBC the object is classified as a methuselah Lazarus comet.

1.1 6478 Gault: Introduction

In the first three months of 2019 five new members have been added to the list of Active Asteroids (AA), one of them, 6478 Gault, with a curious, out of the ordinary tail. In this work we study the phase, secular and rotational light curves of this object.

The discovery of the new main belt comet at the beginning of 2019 was made possible by the Asteroid Terrestrial-Impact Last Alert System, ATLAS, (Smith et al., 2019). The appearance of 6478 Gault immediately called attention because the nucleus did not exhibit a coma and the tail was very long and thin with no evidence of gas. This morphology is quite different from the usual comets that exhibits a gaussian shaped coma and a gas and dust tail that expands and fades with distance to the nucleus. This tail recalls the morphology of 133P/Elst-Pizarro (Hsieh et al., 2004) with which it shares some similar features.

Theoretical interpretations of 6478 Gault (Chandler et al., 2019; Hui et al., 2019; Jewitt et al., 2019; Kleyana et al., 2019; Moreno et al., 2019; Ye et al., 2019), agree that this object is in a state of rotational disruption. Our determination of a rotational period of 3.360 ± 0.005 h supports this conclusion.

6478 Gault is a km-sized asteroid in the Phocaea family (Nesvorny, 2015). Images of 6478 Gault exhibiting its thin, long gas-less tail are shown in Figure 1. Additional images can be found at the following link: <http://www.aerith.net/comet/catalog/A06478/2020-pictures.html>

Some questions we may try to answer are: Is it a sublimating or a suffocating comet? Does it represent a terminal stage in its lifetime? Is there evidence of duplicity?

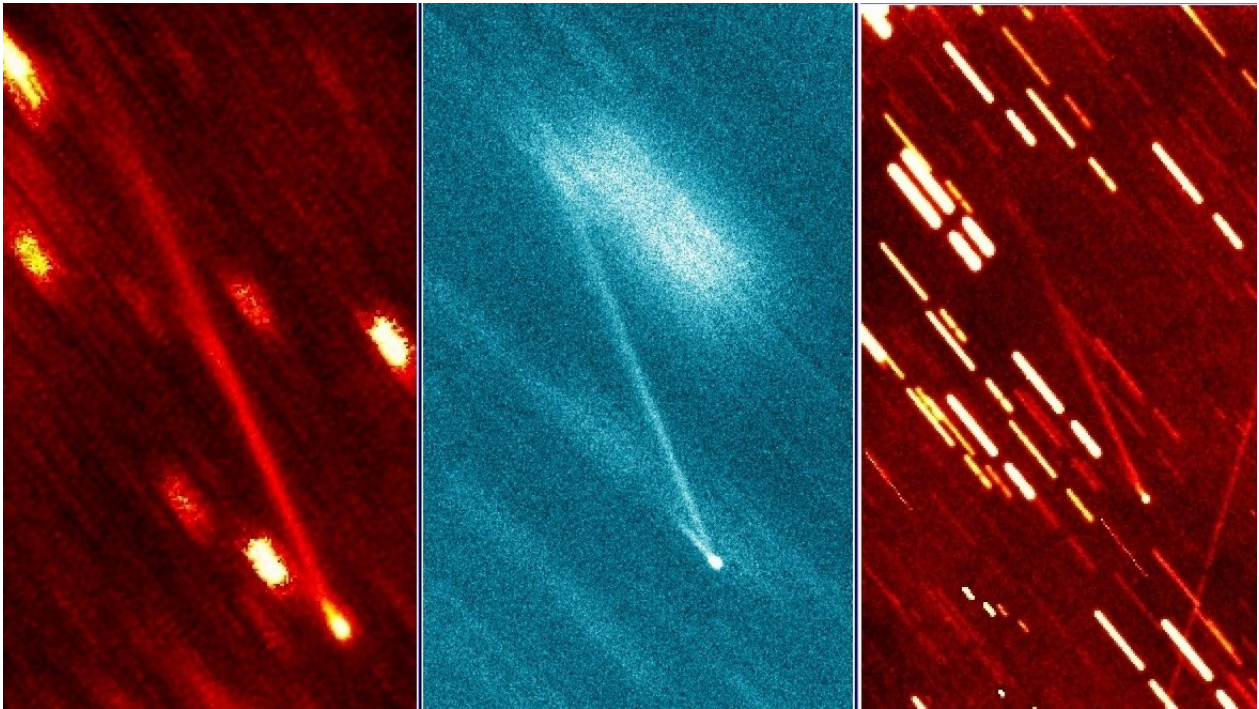


Figure 1. 6478 Gault. **Left image.** Median image of 15 frames x 5 min = 75 min of exposure time, V-band, taken with the 1 m f/5 reflector telescope of the National Observatory of Venezuela, on 2019 02 05. The characteristic features, star-like head, thin, long, gas-less persistent dust tail, and no tail spread as a function of distance, are all exhibited in this object. Tail B, shorter and to the left of the main tail, is compromised by a star. (IF, this work, ONV, CIDA, observatory 303). **Center image.** Image taken with a 35 cm telescope on 2019 02 13 (C. Fornari, observatory X31). 44 images of 5 minutes each were median combined for a total exposure time of 220 min. Tail B is clearly seen. On the original image the ratio length/width > 80. **Right image.** Secured on 2019 02 13 with a 24 cm telescope. 20 images x 5 min = 100 min using average combine (A. Acosta, observatory Z39). The bright patches are stars imperfectly erased by the median.



1.2 6478 Gault: Observations

We carried out photometry of 6478 Gault on 877 images acquired on 41 nights using several telescopes listed in Table 1. The photometry log is listed in Table 2 and values are plotted in Figures 3 and 4. Table 3 contains a list of the parameters derived in this work. We are confident that our photometry is of high quality because we have adopted special procedures in that direction:

- (1) Images were processed with darks and flats in the usual manner.
- (2) We adopt large photometric apertures typically 4-5 FWHM in order to extract the whole flux from the objects.
- (3) We use from 5-15 comparison stars, and reject those that are outliers.
- (4) We use APASS, the best V-magnitude catalog that spans the whole sky, created by the AAVSO to cover the observation of variable stars.

(5) We measure the observed magnitude from long series of images, typically containing 10-50 images with 3-5 minutes of exposure time each, reaching to total exposure times of hours, to plot one single photometric data point per night.

(6) Before combining, each image is examined for defects, cosmic rays, clouds, star contamination, disappearance of the object, reflections and bright stars. Unsuitable images are discarded before combining.

(7) The combination algorithm is the median, to clean up cosmic rays and defects.

(8) Finally, we adopt the envelope of the data points as the correct interpretation of the light curve. The envelope of the data points represents a perfect instrument+CCD, with a perfect atmosphere, capable of extracting the whole flux from the object and thus the maximum relative brightness (Ferrín, 2005).

As a result we routinely achieve an error of ± 0.01 to ± 0.02 magnitudes equivalent to 1-2% error (confirmation Table 2). The error is so small that it is contained inside the plotting symbol in all of our plots.

We also used the MPC observations data base. This database is of lower quality because its photometry is a byproduct of astrometry and several non-photometric catalogs and filters are used. To decrease the scatter and increase the signal to noise ratio, we apply a 5 data point running mean. This way any feature less than 5 data points in length is smoothed out. These values may have to be moved up or down a little bit to fit the high precision photometry of our work.

1.3 6478 Gault: Literature search

There have been 6 articles up to the moment of this writing, related to 6478 Gault. What follows is a resume of some numbers of interest to this investigation, not a review of these complex papers.

(1) Ye et al. (2019) describe two brightening events that start on 2018 October 18 ± 5 d, and a second one that started on 2018 December 24 ± 1 d, and that released 2×10^7 kg and 1×10^6 kg respectively. Each event persisted for about a month. Dust dynamics showed grains of up to 10 microns in size ejected at velocities less than 1 m/s regardless of particle size. Additionally they derive an upper limit to the ejection velocity of < 8 m/s. These ejection events are clearly defined in our Secular Light Curve (Figures 3 and 4, active zones Z1 and Z2).

(2) Kleina et al. (2019) determined an absolute magnitude of 14.4 in the V band based on ~ 1000 survey observations, and with an adopted albedo of 0.04, representative of comets, derive a nucleus 9 km in diameter. They also adopt a density of 3000 kg/m^3 . Although they have an extensive series of observations these did not show a light curve and the rotational period could only be estimated at ~ 1 h for one peak, and ~ 2 h for two peaks. They derived a $v_{\text{eject}} = 0.7$ m/s for the maximum emission velocity.

(3) Moreno et al. (2019) adopt for the dust density 3400 kg/m^3 which is appropriated for S-type asteroids. They also adopt a geometric albedo $p_V = 0.15$ typical of S-types. With an adopted absolute magnitude of $H_V = 14.4$, they find a diameter of 4.5 km. They also apply a phase coefficient of 0.033 mag° . Long series of observations secured with the TRAPPIST-North and South telescopes did not exhibit evidence of a rotational signature.

(4) Jewitt et al. (2019). These authors find mass loss rates of $\sim 10\text{-}20$ kg/s and a typical particle radius in the main tail $\langle a \rangle \sim 1000$ μm . Using the thickness of the tail at the time of orbital plane crossing they are able to calculate a value for the ejection velocity $v_{\text{eject}} \sim 2$ m/s. They also find a close similarity of 6478 to comet 311P/2013 P5 who exhibited multiple dust ejections (Jewitt et al., 2018).

(5) Hui et al. (2019). They confirm the slow dust ejection velocity for the dust, finding $v_{\text{eject}} = 0.15$ m/s. As previous authors they infer that the mass-loss events were caused by rotational instability. They conclude that the two tails observed were caused by the two outburst that were identified in the light curve.

(6) Chandler et al. (2019). They used archival observation to demonstrate that Gault has a long history of previous activity. Their data suggests that activity is caused by a body spinning near the rotational limit. They recognize 6478 as a new class of object perpetually active due to rotational spin up. Their data is plotted in our Figure 3.

It is important to point out that none of the six manuscripts published on this object have a value for the rotational period, thus their conclusions on the reason of activity is entirely theoretical. However this work will validate these conclusions (see Section 2.3). Also, our SLC of 6478 will show that the activity is not perpetual but episodic. The reasons for being episodic are speculative at the present time.

Additional works might be relevant to this investigation.

(7) The conclusion by Hsieh et al. (2004) that “*apparent low ejection velocities of optical dominant dust particles, as implied by the lack of an observable sunward dust extension or coma-like dust halo around the nucleus, and the narrow width of the dust trail, make extremely small particles unlikely to be optically significant*”, in agreement with Jewitt et al. (2019) who also found large particles. These results are consistent with the hypothesis that these large particles are the remnant of the cometary activity deposited on the surface. It is also consistent with the idea that these objects might be completely covered with a thick mantle or dust layer.

(8) Kokotanekova et al. (2017) studied an ensemble of Jupiter-family comets, finding a cut-off in bulk densities at 0.6 g/cm³ if the objects are strength less. They also find an increasing linear phase function coefficient with increasing albedo. Their median linear phase function coefficient for JFCs was 0.046 mag/deg and their median geometric albedo was 4.2% . These values are useful when this information is not available for a given object. We will use their albedo as a lower limit in our calculations.

(9) Hsieh et al. (2009) note that low albedo ($p_R < 0.075$) remains a consistent feature of all cometary (i.e., icy) bodies, whether they originate in the inner solar system (the MBCs) or in the outer solar system (all other comets). We will use their albedo as an upper limit in our calculations.

2.1 6478 Gault: Phase and SLC plots

To advance in our understanding of this object we will make use of the phase plot and the secular light curve (SLCs, Ferrín, 2010a, 2010b). The phase plot shown in Figure 2, does not

exhibit a dependence on phase, implying that the surface is not seen due to an optically thick layer of dust that hides the nucleus. Accordingly no phase correction has been applied to our data. In those cases in which the phase effect is not detected, the absolute magnitude has to be defined using only the SLC plot. The SLC formalism depicts the absolute magnitude of the object versus time, from aphelion $-Q$, to aphelion $+Q$ (Figures 3 and 4). The SLC of 6478 shows evidence of 6 zones of activity, Z1 to Z6. Z1 and Z2 are the outburst studied by (Chandler et al., 2019; Hui et al., 2019; Jewitt et al., 2019; Kleyana et al., 2019; Moreno et al., 2019; Ye et al., 2019).

The origin of these active zones is controversial. It might look like the orbital plane crossings (PCs) are related to the peaks, but this interpretation is not completely convincing. A plane crossing produces an enhancement of the tail lasting typically a few days. However the six zones of activity are much wider than a few days, putting in doubt this interpretation. Active zones Z1 and Z2 may have been the result of an impact.

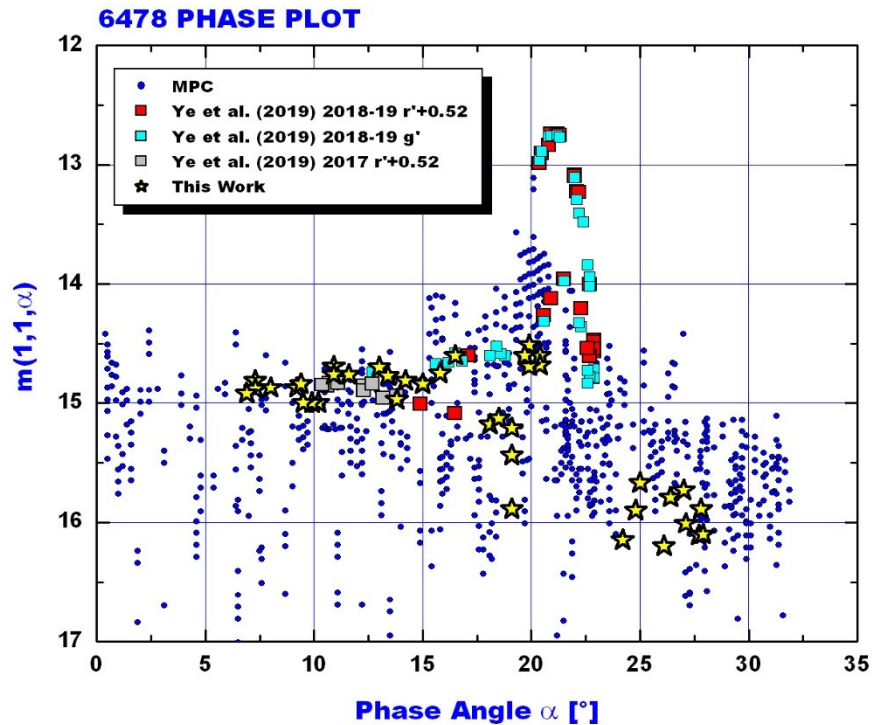


Figure 2 Phase plot of 6478 Gault. The comet does not exhibit a phase effect, implying that we are not seeing the surface. The object must be covered with a cloud of dust that hides the nucleus. That is the reason why we have not applied any phase correction to our observational data. Most of the data show the comet in an excited state, thus to define the absolute magnitude we have to use the SLC plot.

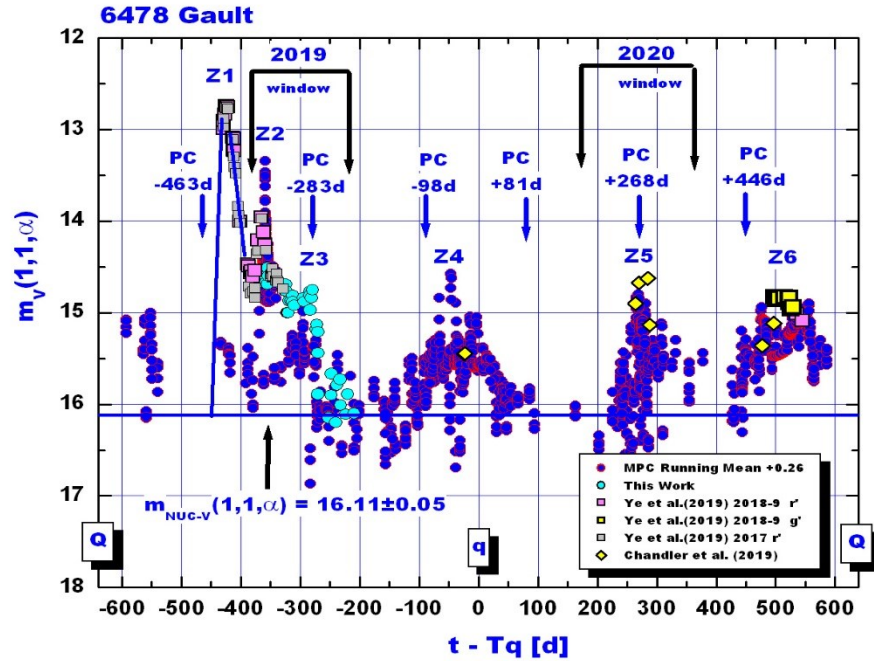
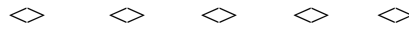


Figure 3. SLC of 6478 Gault. To smooth out the scattering of the data and to increase the signal/noise ratio we applied to the MPC database a 5 data points running mean. Different data sets were combined to create this plot. The absolute magnitudes listed by the Minor Planet Center and the JPL Small Body Database Browser, $H_V= 14.3$ and $H_V= 14.4$ respectively, are too bright. A new value $m_V(1,1,\alpha) = 16.11 \pm 0.05$ is derived in this work using the mean value of our five faintest measurements. Notice that this result is consistent with the faint values at $t-T_q = +160$ d. The object shows 6 zones of activity, Z1 to Z6, the reason for which is not clear at the present time. PC = Orbit Plane Crossing, indicate when the Earth crossed the orbital plane. The plane crossings do not seem to be correlated with the activity zones. Above, the observing windows in 2019 and 2020 are shown. The 2020 window will allow observations of the Z5 zone. Notice that the observations compiled by Chandler et al. (2019) agree quite well with active zones Z4, Z5 and Z6.



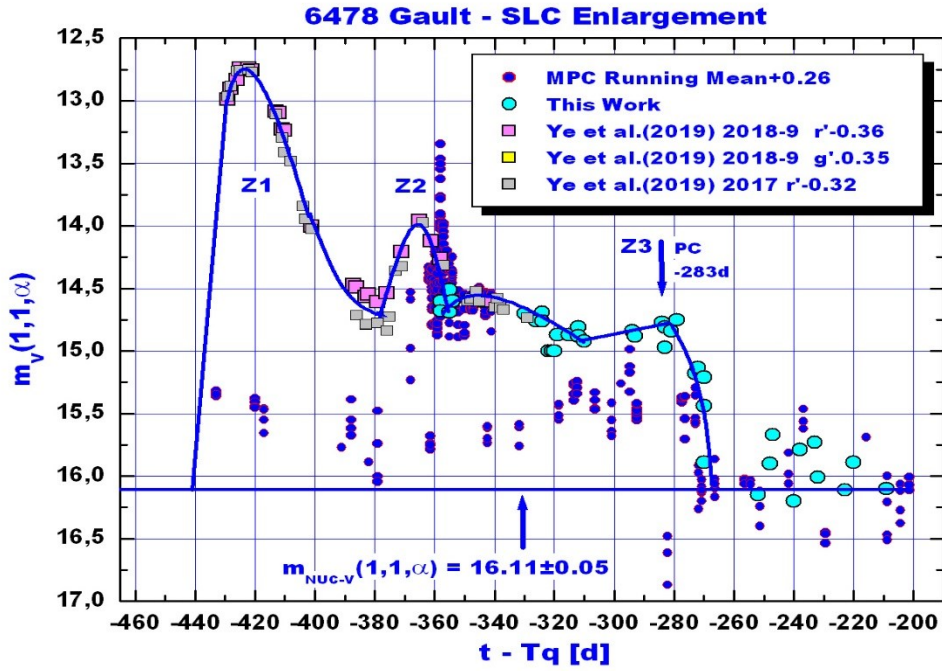


Figure 4. SLC of 6478 Gault. Enlargement of the region -465 d to -200 d before perihelion. The two outburst Z1 and Z2 can be clearly seen and delimited. The average of the 5 faintest measurement gives our best estimate of the absolute magnitude of the nucleus.



2.2 6478 Gault: Absolute Magnitude, Diameter, Mass

Absolute magnitude. The SLC plot gives the whole picture from $-Q$ to $+Q$ (Q = aphelion distance) needed to select a reliable absolute magnitude. The $m_v(1,1,0)$ and the observed magnitude $m_v(\Delta, R, \alpha)$ are related by

$$m_v(1,1,0) = m_v(\Delta, R, \alpha) - 5 \cdot \text{Log}(\Delta \cdot R) - \beta \cdot \alpha \quad (1)$$

where Δ is the object-Earth distance, R the Sun-object distance, α is phase angle and β the phase coefficient. A reduction law more sophisticated than a linear law is not justified because the phase angle does not exceeds 33° .

In Figures 3 and 4, the SLC plot, five data points have the lowest values of the dataset, 16.15, 16.20, 16.01, 16.10, and 16.11. The range is 0.19 in excellent agreement with the amplitude of the rotational light curve found later on ($\text{Amp} = 0.16 \pm 0.02$) (see Section 5.3). The mean value is our best estimate of the absolute magnitude, $m_v(1,1,\alpha) = 16.11 \pm 0.05$.

The works cited in Section 1.3 adopted for their calculations an absolute magnitude 1.71 magnitudes brighter than our result. Consequently some of the model calculations performed in the above works might have to be revised.

Diameter. With this information it is possible to calculate the diameter D if the geometric albedo, p_v , is assumed. Jewitt (1991) gives the following formula

$$p_v r(\text{nuc})^2 = 2.24 \times 10^{22} \cdot R^2 \cdot \Delta^2 \cdot 10^{[0.4(m_{\text{SUN}} - m_v(1,1,0))]} \quad (2)$$

which can be written in a more amicable form

$$\text{Log} [p_v \cdot D^2 / 4] = 5.654 - 0.4 m_v(1,1,0) \quad (3)$$

Kokotanekova et al. (2017) calculated a mean geometric albedo of the Jupiter Family of comets $\langle p_v \rangle = 0.042 \pm 0.005$. Since the SLC of 6478 indicates that the object is behaving more like a comet than an asteroid, we are going to adopt this value in our calculations. Then we find for the diameter $D = 3.93 \pm 0.25$ km, $r = 1965 \pm 125$ m. Hisieh (2009) gives a maximum $p_v = 0.075$. If we use this value we find $D = 2.94$ km, $r = 1470$ m.

Mass. To calculate the mass we need a density. Later on we will find a rotational period for Gault $\text{Prot} = 3.360 \pm 0.005$ h and an amplitude $\text{Amp} = 0.16 \pm 0.02$, which translates to a ratio of axis $a/b = 1.16$. In the Section on rotation (Section 2.3) we calculate that the minimum density to hold material at the tip of this rotating asteroid is $P_{\text{CRITICAL}} \sim 1120$ kg/m³. Then the estimated mass of the nucleus is $M_{\text{NUC}} = (3.6 \pm 0.35) \times 10^{13}$ kg for $\langle p_v \rangle = 0.042$ or $M_{\text{NUC}} = (1.5 \pm 0.25) \times 10^{13}$ kg for $\langle p_v \rangle = 0.075$.

The masses ejected calculated by the previous researchers were very small, 2 to 4×10^7 and 1×10^6 kg for active zones Z1 and Z2 (Ye et al., 2019; Jewitt et al., 2019). If this mass were to be released by apparition and sustained in time, the number of returns left would be $\sim 18,000$. If this mass were spread out uniformly over the surface, the depth of the layer would be only 0.4 mm. This information combined with the negative detection of a phase effect implies that there is a deep layer of dust on this surface which is quenching the sublimation activity.

2.3 6478 Gault: Rotational Period

An attempt to measure the rotational period was made by Kleyna et al. (2019) who found a value ~ 2 h. However phasing and smoothing of their data did not reveal any obvious light curve, suggesting that the periodic signal was buried in aperiodic, non-Gaussian noise.

We used the 24 cm telescope of Z39 to take 178 observations of asteroid-comet 6478 Gault and processed them with software Canopus and Maxim-DL to measure the rotational period of this object (Ferrín and Acosta, 2019) (the data is listed in Table 6). We observed 6478 from January 12th to April 8th during 8 nights and used a 5 data point running mean to diminish the scattering of the data and to increase the signal to noise ratio by a factor of 2.2. Since this average operates only in the vertical direction there is no way it can modify the period. The NASA Exoplanet periodogram tool was used to calculate the period with the Lomb-Scargle option. To our surprise the periodogram found a period around ~ 0.07 d corresponding to rotational light curve with one peak and $\text{Prot}(1) = 1.680 \pm 0.002$ h and amplitude $\text{Amp}(1) = 0.180 \pm 0.002$ mag. And with two peaks, $\text{Prot}(2) = 3.360 \pm 0.005$ h and amplitude $\text{Amp}(2) = 0.16 \pm 0.02$. The periodogram is shown in Figure 5.

It is interesting to point out that we did not expect that the 24 cm telescope could find a period for this 17-magnitude target, but it did. There is no way in which this result could have been falsified. Each observation corresponds to a phase in the phase curve, and the observer does not have any way to know the phase for any observing night. The only thing he can do is secure the observations and hope for the best. So if the software finds a period and the period produces a reasonable light curve, it must be real. As a confirmation, the light curve produced looks quite robust (Figures 6 and 7) and has been confirmed (Figure 8).

The first period with one rotational peak violates the rotational limit for disruption of a rubble pile asteroid (~ 2.2 h) (Jewitt et al., 2014), so we adopt the second one with two rotational peaks. A 0.16 mag amplitude corresponds to a ratio of axis $a/b=1.16$. The minimum density needed to ensure the material at the tip of a prolate body in rotation about its minor axis that is gravitationally bound is given by Jewitt et al. (2014)

$$\rho_{\text{CRITICAL}} \sim 1000 (3.3/\text{Prot})^2 [a/b] \quad (4)$$

If we use the observed period, 3.360 h and the observed ratio $a/b=1.16$ then the minimum density comes out to be $\rho_{\text{critical}} > \sim 1.12 \text{ gm/cm}^3$, a very reasonable value expected for a comet mainly made of water ice.

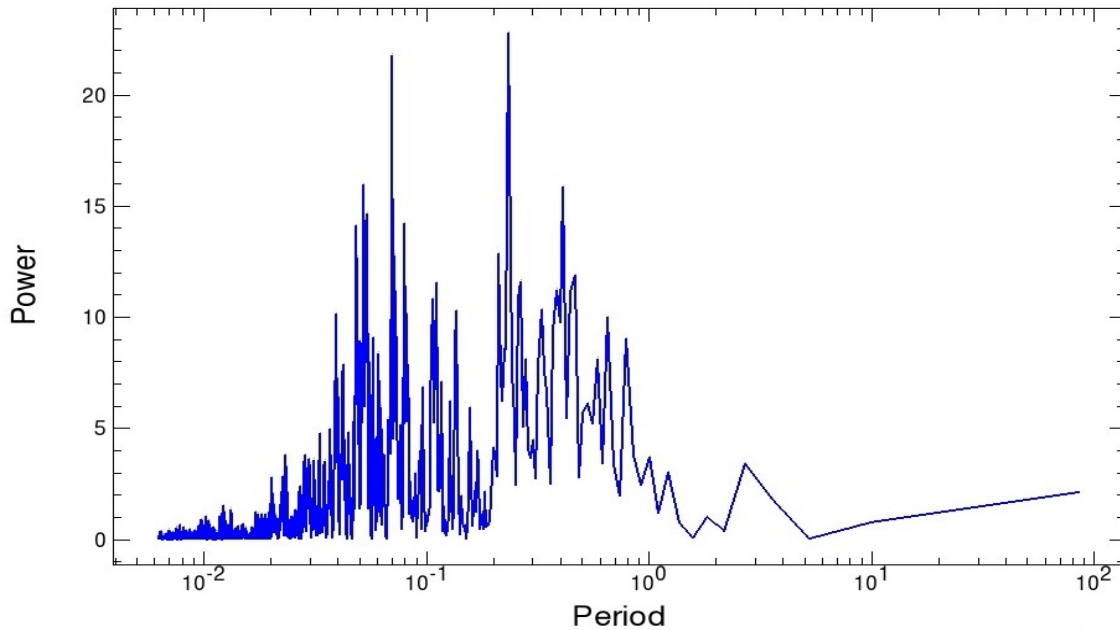


Figure 5. The periodogram of 6478 Gault shows two main peaks at periods ~ 0.07 d and ~ 0.23 days. The peak at $\sim 0.23 = 5.52$ h gives a light curve of poor quality so it is not considered further. Peak 1 with one rotational peak corresponds to $\text{Prot}(1)=1.680\pm 0.002$ hours and with two peaks corresponds to $\text{Prot}(2)=3.360\pm 0.005$ hours. The amplitudes are $\text{Amp}(1) = 0.18\pm 0.02$ and $\text{Amp}(2) = 0.16\pm 0.02$ magnitudes respectively. The first one with one rotational peak violates the rotational limit for disruption, so we adopt the second one with two rotational peaks. This plot was generated by the periodogram tool of the NASA Exoplanet page.

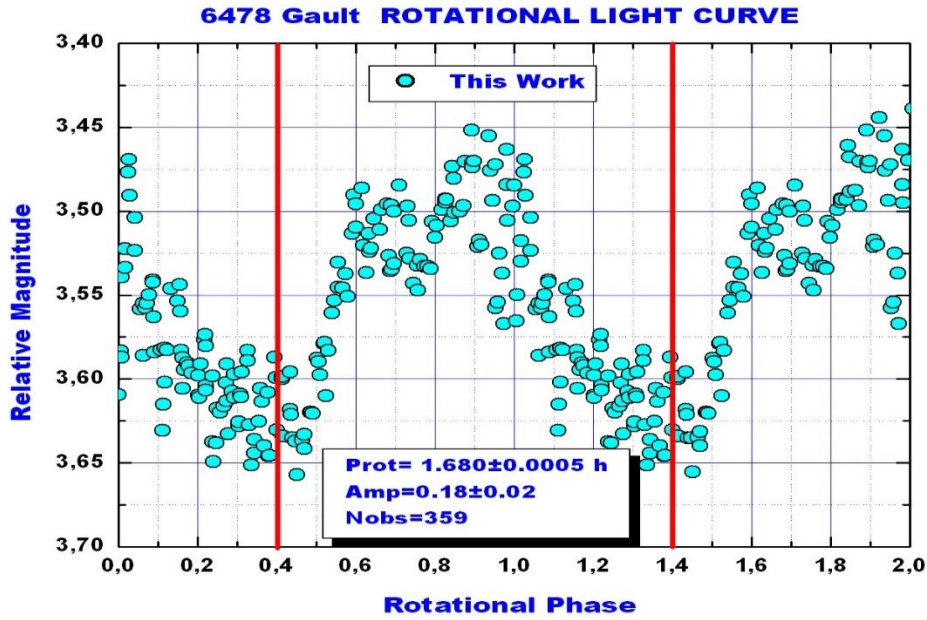


Figure 6. The first solution for the rotational period of 6478 Gault uses one single maximum with period $\text{Prot}(1)=1.680\pm 0.002$ hours and amplitude $\text{Amp} = 0.18\pm 0.02$ magnitudes but violates the rotational limit for disruption (~ 2.2 hours).

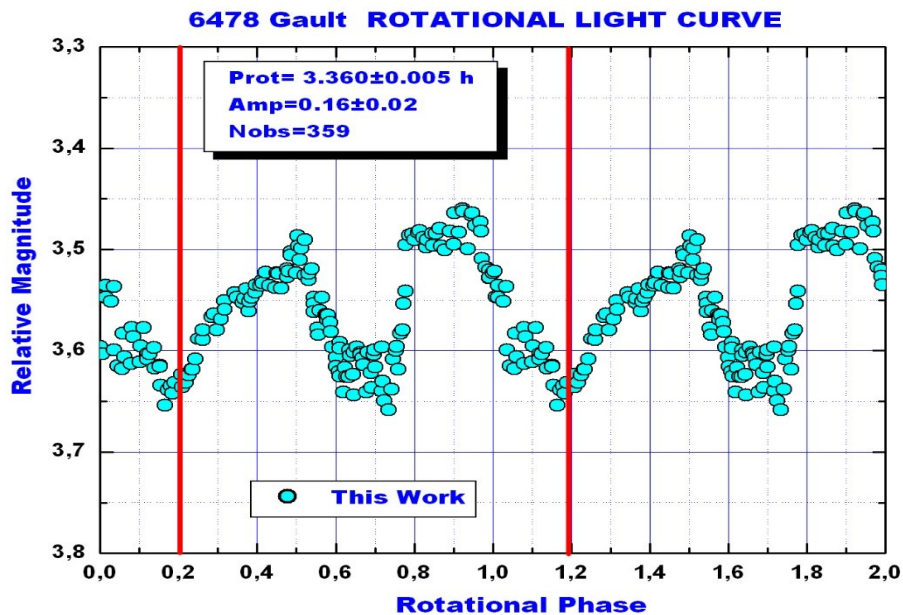


Figure 7. The second solution for the rotational period of 6478 Gault shows two rotational peaks and a rotational period $\text{Prot}(2) = 3.360\pm 0.005$ hours with amplitude $\text{Amp}(2) = 0.16\pm 0.02$ magnitudes.

In Table 4 we list the rotational periods of Gault, 133P/Elst-Pizarro and 62412. We see that all of them have almost identical rotational periods. Since they exhibit the same tail morphology of 6478, implies that these objects are in a state of rotational disruption too.

2.4 6478 Gault: Eclipse

Surprisingly the phased light curve diagram shows evidence of an eclipse in the form of a flat bottom V (Figure 7), with the following de-trended values $T1(\text{phase}, \text{mag}) = (0.53, 0.0) = 190$ deg, $T2 = (0.62, 0.13) = 223$ deg, $T3 = (0.74, 0.13) = 266$ deg, $T4 = (0.80, 0.0) = 288$ deg, $T4 - T1 = 0.27 = 97$ deg, $T3 - T2 = 0.12 = 43$ deg, $(T1 + T2 + T3 + T4)/4 = 0.673$, $m3 - m1 = 0.13$ mag (Figure 8).

To produce a flat bottom the two components have to have different sizes with radii of the primary and secondary, r_p and r_s . Assuming spheres and equal albedos we find the area projected by both components

$$A_{\text{Max}} = \pi \cdot (r_p^2 + r_s^2) \quad (5)$$

$$A_{\text{min}} = \pi \cdot r_p^2 \quad (6)$$

The duration of the eclipse is $T4 - T1 = 0.907$ h and it must correspond to a distance $v \cdot (T4 - T1) = 2 \cdot (r_p + r_s)$, thus we can calculate the projected space velocity. Kepler's third law agglutinates a number of measurable parameters assuming circular orbit of radius a around the primary (Jewitt et al., 2018):

$$a = 4 \cdot \pi \cdot G \cdot \rho \cdot (r_p^2 + r_s^2) / (3 \cdot v^2) \quad (7)$$

A preliminary analysis depends on the absolute magnitude value of the object and requires selecting two free parameters, the geometric albedo, p_v , and the density, ρ . For the geometric albedo we are going to adopt the limits set by Kokotanekova et al. (2017) (~ 0.042) and Hisieh et al. (2009) (< 0.075). For the density we are going to adopt the minimum critical value derived from the rotational parameter (1120 kg/m^3). The solution for a contact binary requires an additional condition,

$$(r_p + r_s) = 2 \cdot a \quad (8)$$

Solving equations (5), (6), (7) and (8) with $p_v = 0.042, 0.06, 0.075$, we find a radius of the primary 1850 m, 1550 m, 1390 m, and for the secondary 660 m, 552 m and 495 m. In order to get these results a minimum density of 1590 kg/m^3 has to be adopted. If the density increases above this value the pair is detached.

The observational projected space velocities are $v_{\text{rot}} = 1.54, 1.28, 1.15$ m/s in very good agreement with the theoretical scape velocity of the dust $0.7 - 8$ m/s (Chandler et al., 2019; Hui et al., 2019; Jewitt et al., 2019; Kleyna et al., 2019; Moreno et al., 2019; Ye et al., 2019).

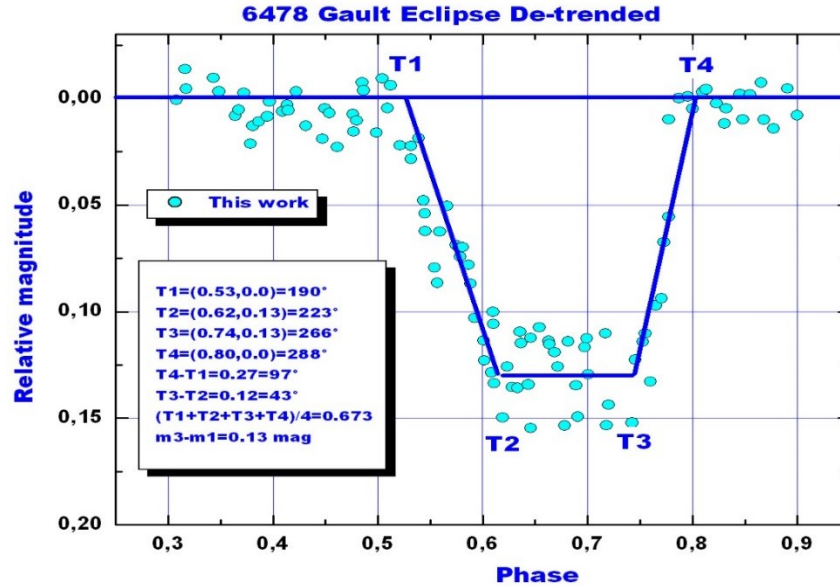


Figure 8. De-trended Eclipse in the light curve of 6478 Gault. The four eclipse parameters, T1, T2, T3 and T4 are listed in the inset table. The total eclipse lasted for $(T4-T1) \cdot \text{Prot} = 0.907$ hours. The deduced physical parameters of the double nucleus are calculated in the text.



2.5 6478 Gault: Confirmation of the rotational period

Carbognani and Buzzoni (2019) were able to reproduce our result (Figure 9). They used the 80 cm Telescope of the Osservatorio Astronomico della Regione Autonoma della Valle d'Aosta, Associato al INAF (Osservatorio Astronomico di Torino, Italy). We applied a 5 data point running mean to their data to increase the signal to noise ratio. They found a period of 3.358 h in excellent agreement with our result. However the eclipse is no longer evident, leaving the object with one single minimum per rotation, clearly an albedo feature.

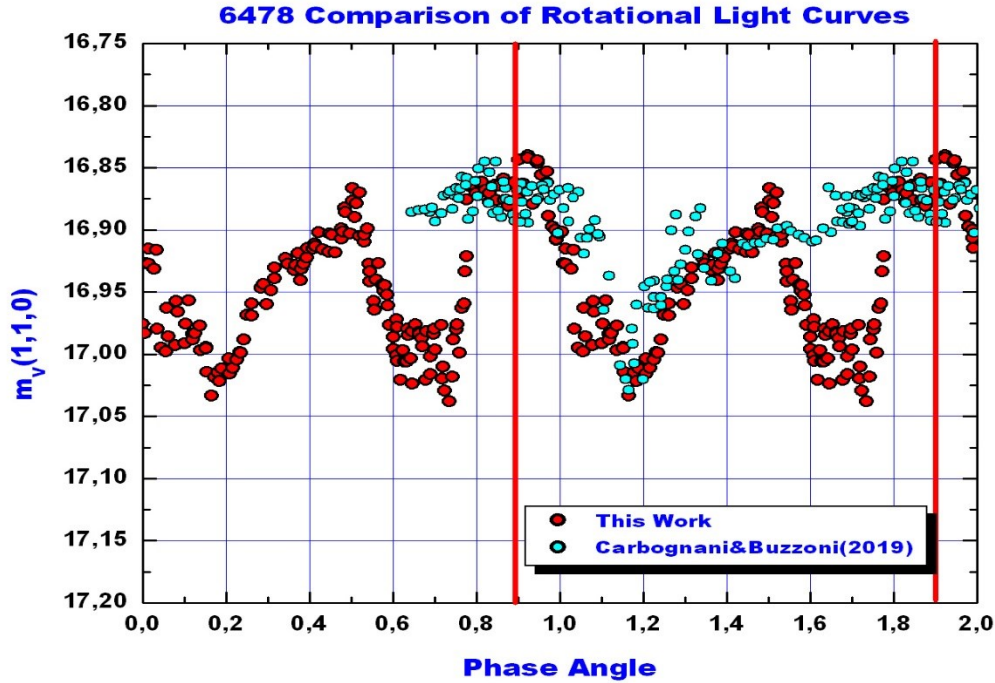


Figure 9. The rotational light curve of Carbognani and Buzzoni (2019) is compared with our rotational light curve. They found a period of 3.358 h vs 3.360 hour for our work. The agreement is satisfactory. The principal distinction is that the eclipse feature has disappeared. Then the light curve can not be that of an elongated body because it would exhibit two peaks. The new interpretation is of an almost spherical nucleus with a zone of lower albedo, producing one single minimum per revolution.



3. 6478 Gault: Discussion and Current Understanding

From the previous works (Chandler et al., 2019; Hui et al., 2019; Jewitt et al., 2019; Kleyna et al., 2019; Moreno et al., 2019; Ye et al., 2019), all of which agree on a basic understanding of this object, and with the results presented in this investigation, the following picture emerges, and this picture may be shared with two other objects, 133P/Elst-Pizarro (Hsieh et al., 2004) and 62412 (Sheppard and Trujillo, 2014) (Tables 4 and 5).

Comets expel gas and dust from their surfaces during their lifetimes. Fine dust is carried away by the gas, but large dust falls down onto the surface creating a dust mantle that increases in thickness with time. At the same time that this process is taking place, the majority of cometary nucleus are increasing their rotational frequency due to offset gas jets that exert a torque on the nucleus diminishing its rotational period and increasing its angular momentum. After many returns around the Sun, the dust mantle increases in thickness and there comes a moment when the mantle quenches the cometary activity creating a dormant comet (Snodgrass et al., 2017).

The comet will remain in this stage if the perihelion distance is kept the same or if it increases in distance to the Sun. But the dormancy can be broken if the perihelion distance decreases, creating a thermal wave that will penetrate deeper into the nucleus reactivating the activity. The comets with decreasing perihelion distance and increasing activity have been designed as Lazarus comets. A good example of a Lazarus comet is 107P/Wilson-Harrington (Ferrín, 2013).

Among these old comets there may be a small group that due to the spin up may have rotational periods near the rotational limit (Hsieh et al., 2014; Jewitt et al., 2018). These objects would emit dust into space, expelled at very small ejection velocities by centrifugal forces, but would not show evidence of gas. It is believed that this is the mechanism that expelled the dust off the surface of these objects.

Due to the thick layer of dust accumulated on the surface, the activity is quenched or suffocated. By expelling dust into space, the dormant comet is actually getting rid of the suffocation. Thus our conclusion is that 6478 Gault is a suffocated comet getting rid of its suffocation by expelling surface dust into space using centrifugal forces. This is an evolutionary stage in the lifetime of some comets.

4. 6478 Gault: Age

It would be interesting if we could assign an age to this comet. We can define a proxy for age based on the amount of mass lost per apparition (Ferrín, 2014). The argument is that as they age the amount of mass expelled diminishes with time. Thus a proxy for age may be the inverse of the apparition mass loss. The proposed definition is

$$\text{ML-Age [cy]} = 3.58 \times 10^{11} \text{ kg} / \text{Mass Loss per Apparition} \quad (9)$$

where cy stands for comet years, different from Earth's years, and the constant was chosen so that comet 28P/Neujmin 1 has an age of 100 cy. For the two initial outbursts Ye et al. (2019) calculate masses released 2.7×10^7 kg and 1×10^6 kg, while Moreno et al. (2019) find 1.4×10^7 and 1.6×10^6 kg. For the first outburst Hui et al. (2019) find 9×10^6 kg. If we first take the average of these values and then scale them to the whole apparition we estimate an apparition mass loss of 2×10^7 kg. Applying Equation (9) we find $\text{ML-Age(Gault)} \sim 18000$ cy. Any object above 100 cy is a Methuselah comet (Ferrín, 2014), thus this is a very evolved object.

5. Future Evolution

The activity of 6478 Gault depends on the total amount of energy received from the Sun. In Figure 10 we show the solar insolation due to perihelion distance changes from 1900 to 2100. The energy received depends on the inverse of the perihelion distance squared, normalized to the year 2020 ($= 1 = 100\%$). We see that the perihelion distance has a secular decrease, causing a secular increase in energy input from the Sun, and classifying this object as a Lazarus comet. The conclusion is that the current activity will remain quite stable, increasing secularly at a rate of only +0.002 % per year.

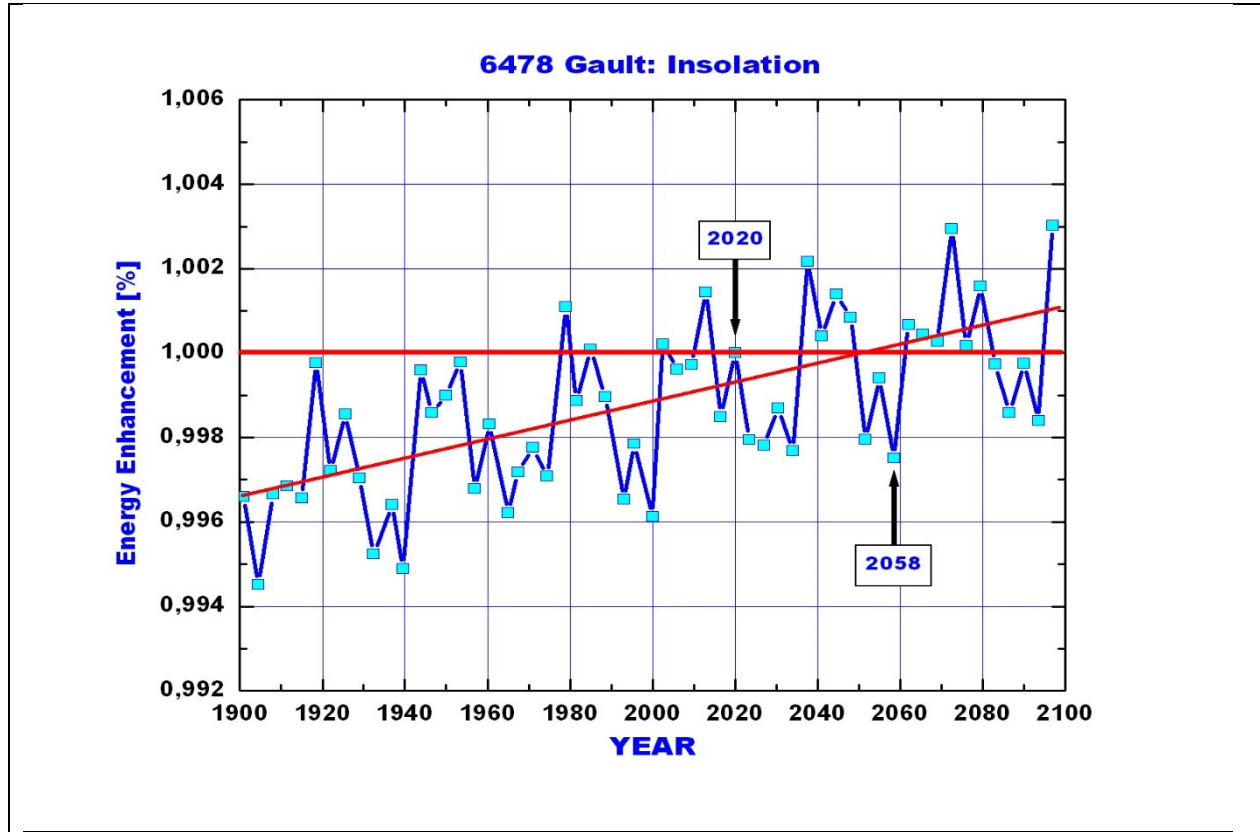


Figure 10. 6478 Gault: insolation . The small vertical variation of the energy received from the Sun indicates that the orbit and energy budget of this object is quite stable in the time range covered by this plot (1900-2100). The small decrease from 2020 to 2058 (+0.02%) will not be sufficient to quench the activity, thus we expect to see 6478 active in the coming apparitions. The tilted line indicates a secular increase in solar insolation due to a diminution of perihelion distance, classifying this object as a Lazarus comet.



6. Conclusions

(1) We present the phase curve of this object and find that there is no phase effect. We interpreted this as due to an optically thick cloud of dust covering the nucleus and hiding the surface.

(2) The SLC of this object exhibits the existence of six zones of activity which complicate the understanding of its secular activity. An explanation based on the orbital plane crossing is not entirely satisfactory, thus the reason for 6 active zones is speculative. Zones 1 and 2 might have been due to an impact.

(3) We determine the absolute magnitude of 6478 as $m_V(1,1,\alpha) = 16.11 \pm 0.05$.

(4) We determined the rotational period of the object. The periodogram shows one period $\text{Prot}(1)=1.680\pm 0.002$ hour with one single rotational peak of activity that violates the rotational limit for disruption (~ 2.2 hours) and is rejected. Doubling that period we get $\text{Prot}(2)= 3.360\pm 0.005$ hours with two rotational peaks of activity, is similar to the rotational periods of comets 133P/Elst-Pizarro (3.471 h) and 62412 (3.33 h) to which it resembles. The $\text{Amp}(2) = 0.16\pm 0.02$ magnitudes.

(5) These objects are in a state of flux. Their changing perihelion distance modifies the amount of energy received from the Sun. In the case of 6478 the perihelion distance is decreasing secularly and thus the insolation is increasing although at a very slow pace. Thus the comet is rejuvenating and classified as a Lazarus comet.

(6) Our rotational period for 6478 Gault was confirmed by Carbognani and Buzzoni (2019) who found a rotational period $\text{Prot} = 3.358\pm 0.005$ hours in excellent agreement with our result. However in their light curve the eclipse is no longer visible, leaving the light curve with one single minimum per rotation. This suggests a spherical shape with one single dark region.

(7) Using a proxy for age, we calculate that this object has a ML-Age ~ 18000 cy (comet years). Any object above 100 cy is a Methuselah comet (Ferrín, 2014), thus this is a very evolved object.

(8) Our conclusion is that 6478 Gault is a suffocated comet getting rid of its suffocation by expelling surface dust into space using centrifugal forces. This is an evolutionary stage in the lifetime of some comets.

(9) We can answer the questions we asked at the introduction: Is it a sublimating or a suffocating comet? It is a suffocated comet that is getting rid of its suffocation by means of centrifugal forces. Does it represent a terminal stage in its lifetime? Yes. Some comets evolve into this stage. Is there evidence of duplicity? Yes. The light curve showed evidence of an eclipse.

(10) Besides being a MBC this object is classified as a methuselah Lazarus comet.

7. Acknowledgements

The FACom group is supported by the project ‘Estrategia de Sostenibilidad 2015–2016’, sponsored by the Vicerectoría de Investigación of the Universidad de Antioquia, Medellín, Colombia. This work contains observations made at the National Observatory of Venezuela, ONV, Centro de Investigaciones de Astronomía, CIDA, Mérida. The help of Giuliatna Navas and the night assistants The FACom group is supported by the project ‘Estrategia de Sostenibilidad 2015–2016’, sponsored by the Vicerectoría de Investigación of the Universidad de Antioquia, Medellín, Colombia. Richard Rojas, Leandro Araque, Dalbare Gonzalez, Fredy Moreno, Carlos Pérez, Gregory Rojas, Daniel Cardozo and Ubaldo Sánchez, is particularly appreciated. We used as comparison stars the APASS catalogue published by the AAVSO. We acknowledge with thanks the comet observations from the COBS Comet Observation Database, contributed by observers worldwide and used in this research. The contribution of images by Jesús Canive, Edwin Quintero and José Francisco Hernández is appreciated.

8. References

- Carbognani, A., Buzzoni, A., (2019). MNRAS, submitted.
- Chandler, C. O., Kueny, J., Gustafsson, A., Trujillo, C. A., Robinson, T. D., Trilling, D. E., (2019). Six years of sustained activity from Active Asteroid (6478) Gault. *Ap. J. Letters*, 877, L12, 9 pp..
- Ferrín, I., “Variable aperture correction method in cometary photometry”, (2005). *ICQ*, October, 249-255.
- Ferrín, I., "Atlas of secular light curves of comets", 2010. *PSS*, 58, 365-391.
<http://arxiv.org/ftp/arxiv/papers/0909/0909.3498.pdf>
- Ferrín, I., Zuluaga, J., Cuartas, P., (2013). The location of Asteroidal Belt Comets (ABCs) On a comet’s evolutionary diagram: The Lazarus Comets. *MNRAS*, 434, 1821-1837.
- Ferrín, I., Acosta, A., 6478 Exhibits a Rotational Period of 3.36 hours and Might be Double (2019). *Astronomer's Telegram*, #12663.
- Hsieh, H., Jewitt, D. C., Fernandez, Y., (2004). The Strange Case of 133P/Elst-Pizarro, A Comet Among the Asteroids. *An. J.*, 127, 2997-3017.
- Hsieh, H., Jewitt, D. C., Fernandez, Y., (2009). Albedos of Main-Belt Comets 133P/Elst-Pizarro and 176P/Linear. *Ap. J.*, 694, L111.
- Hui, M., Kim, Y., Gao, X., (2019). New Active Asteroid (6478) Gault.
<https://arxiv.org/pdf/1903.09943.pdf>
- Jewitt, D., Weaver, H., Mutchler, M., Li, J., Agarwal, Jessica, Larson, S., (2018). The Nucleus of Active Asteroid 311P/(2013 P5) PANSTARRS. *An. J.*, 155, 231, 11pp.
<https://arxiv.org/pdf/1804.05897v1.pdf>
- Jewitt, D., Kim, Y., Luu, J., Rajagopal, J., Kotulla, R., Ridgway, S., Liu, W., (2019). Episodically Active Asteroid (6478) Gault. *Ap. J., Letters*, 876, L19, (11pp).
<https://arxiv.org/pdf/1904.07100.pdf>
- Kleyna, J. T. et al. (2019) The Sporadic Activity of (6478) Gault: A YORP – driven event? *Ap. J.*, 874, L20 (7pp). <https://arxiv.org/pdf/1903.12142v1.pdf>
- Kokotanekova, R., Snodgrass, C., Lacerda, P., Green, S. F., Nilolov, P., Bonev, T., (2017). Rotation of Cometary Nuclei: New Lightcurves and an Update of the Ensemble Properties of Jupiter-Family Comets. *MNRAS*, 471, 2974-3007.
<https://arxiv.org/pdf/1707.02133.pdf>

- Moreno, F., and 13 colleagues, (2019). Dust Properties of Double-Tailed Active Asteroid (6478) Gault. *A&A*, 624, L14 (11pp). <https://arxiv.org/pdf/1903.09943.pdf>
- Nesvorny, D., (2015). *NASA Planetary Data System*, 234, EAR.
- Sheppard, S. S., Trujillo, C., (2014). Discovery and Characteristics of the Rapid Rotating Active Asteroid (62412) 2000 SY178 in the Main Belt. *An. J.*, 149, 44, 9pp.
- Smith, K., Denneau, L., Vincent, J. B., Weryk, R., (2019). CBET 4594
- Snodgrass, C., and 13 colleagues. *Main Belt Comets and Ice in the Solar System*, (2017). *A&A Review*, 25, p. 5.
- Ye, Q., and 15 colleagues, (2019). Multiple Outbursts of Asteroid (6478) Gault. *Ap. J.*, 874, (8pp). <https://arxiv.org/pdf/1903.05320.pdf>.

TABLES**Table 1.** Instrumentation

Observatory	MPC Code	City	Country	Diameter	CCD	Observer
Galileo Galilei Lat-31°49'22.96" Lon60° 31' 14.3"	X31	Oro Verde Entre Rios	Argentina	35 cm	Sbig 8300M	Cesar Fornari
Costa Teguisse Lat +28° 59 45.8 Lon 13° 30' 04.7 W Alt 37 m	Z39	Lanzarote, Canary Islands	Spain	24 cm	ST-8XME	Agustin Acosta
CIDA Lat 8° 47' Lon 70° 52' W Alt 3590 m	303	Merida	Venezuela	100 cm	Techtronic	Ignacio Ferrín
Ibiernes Lat 41° 05' 51" Lon -02° 34' 22" Alt 1058 m	-----	Gujosa	Spain	30 cm	RC 12" F8 SBIG STL 1301 3 CCD	Jesus Canive
Altamira Lat +28° 14' 46" Lon -16° 26' 32" Alt 589 m	X05	Fasnia, Canary Islands	Spain	40 cm	1336x890 SBIG STL- 11000 3 CCD	José Francisco Hernández Quico
Tecnological University of Pereira Lat +04° 47' Lon 75° 41' Alt 1533 m	W63	Pereira	Colombia	40 cm	SBIG ST2000	Edwin Quintero

Table 2. Observing log of 6478 Gault

YYYYMMDD	$m_V(1,1,0)$	t-Tq [d]	Observer	#images
190110	14.60±0.04	-358	Acosta	6
190110	14.68±0.04	-358	Acosta	11
190113	14.51±0.03	-355	Acosta	18
190113	14.69±0.03	-355	Acosta	14
190114	14.60±0.03	-354	Acosta	14
190127	14.60±0.03	-341	Acosta	10
190207	14.70±0.02	-330	Acosta	19
190205	14.73±0.02	-328	Ferrín	15
190211	14.76±0.03	-326	Acosta	16
190213	14.69±0.01	-324	Acosta	19
190213	14.76±0.01	-324	Acosta	19
190215	15.00±0.01	-322	Fornari	18
190216	15.00±0.01	-321	Fornari	21
190217	15.00±0.01	-320	Fornari	23
190218	14.87±0.01	-319	Fornari	17
190222	14.87±0.01	-315	Fornari	35
190225	14.81±0.02	-312	Acosta	43
190225	14.88±0.02	-312	Fornari	12
190227	14.92±0.02	-310	Fornari	44
190315	14.84±0.01	-294	Acosta	11
190316	14.88±0.01	-293	Acosta	56
190325	14.77±0.02	-284	Fornari	11
190326	14.97±0.01	-283	Fornari	20
190327	14.81±0.01	-283	Acosta	35
190329	14.84±0.02	-281	Acosta	31
190331	14.75±0.01	-279	Hernández	24
190406	15.18±0.02	-273	Acosta	17
190407	15.13±0.01	-272	Acosta	16
190409	15.44±0.02	-270	Fornari	16
190409	15.89±0.01	-270	Acosta	36
190409	15.21±0.01	-270	Hernández	9
190427	16.15±0.02	-252	Acosta	7
190430	15.90±0.01	-248	Fornari	21
190501	15.67±0.02	-247	Fornari	27
190508	16.20±0.05	-240	Canive	10
190510	15.79±0.02	-238	Canive	11
190515	15.73±0.02	-233	Canive	8
190516	16.01±0.01	-232	Fornari	31
190525	16.11±0.01	-223	Fornari	11
190528	15.89±0.02	-220	Quintero	5
190608	16.10±0.05	-209	Fornari	17

Table 3. Physical parameters of 6478 determined in this work.

object	m110	D [km] r [m]	Asec(q)	Δt (active) [d]	β [mag/°]
133P	15.83±0.05	4.2±0.8	-2.4±0.01	150	0.044
6478	16.11±0.05	3.9	~-1.4 ¹	~200	0.0

1- 6478 has several zones of activity, Z1-Z6. Excluding Z1 and Z2 that might be the result of an impact, the others have a typical amplitude of ~-1.4 mag and duration ~200 d.

Table 4. Rotational Periods

Object	Rotational Period [h]	Reference
133P	3.471	Hsieh et al. (2014)
6478	3.360±0.005	This Work
62412	3.33	Sheppard and Trujillo (2010?)

Table 5. Orbital Elements and Tisserand Parameter of 133P, 6478 and 62412

Asteroids have $T_J > 3.0$; Comets of the Jupiter Family have $2.0 < T_J < 3.0$

OBJECT/ FAMILY	q[AU]	Q[AU]	e	i[°]	a[AU]	Tq yyyymmdd	Porbit [y]	class Tiss
6478 Gault	1.86	2.75	0.19	22.8	2.30	2020 01 03	3.5	Phocaea 3.461
133P	2.66	3.66	0.16	1.39	3.16	2018 09 21	5.62	Themis 3.185
62412	2.90	3.40	0.81	4.73	3.15	2018 10 29	5.59	Hygeia 3.197

Table 6. Rotational plot: measurements.

Time	mag	Time	mag	Time	mag	Time	mag
496.58051	3.6396	539.49945	3.5968	559.50057	3.5426	580.36882	3.5621
496.58436	3.6436	539.50329	3.5851	559.50371	3.5721	580.37132	3.5426
496.58833	3.6188	539.50713	3.5744	559.50684	3.4772	580.37382	3.5012
496.59217	3.6538	539.51097	3.5646	559.50999	3.5062	580.37632	3.5426
496.59603	3.6152	539.51482	3.4938	559.51314	3.5126	580.37881	3.5478
496.59987	3.5902	539.51866	3.5126	559.51628	3.5162	580.38131	3.5776
496.60371	3.6111	539.52251	3.5568	559.51941	3.5248	580.38381	3.6028
496.61308	3.6202	539.52633	3.4782	559.52255	3.5288	580.38631	3.6476
496.62809	3.5922	539.53016	3.4281	559.52569	3.4816	580.38881	3.5768
496.63193	3.5991	559.36165	3.4562	559.52882	3.4931	580.39129	3.5876
496.63576	3.5521	559.36515	3.4278	559.53196	3.5104	580.39378	3.5972
496.63959	3.5308	559.36831	3.3998	559.53511	3.4336	580.39628	3.5838
496.64342	3.5758	559.37145	3.5261	559.56333	3.3884	580.39877	3.5772
496.64726	3.5451	559.37461	3.6042	559.56647	3.3462	580.40127	3.6552
496.65109	3.5684	559.37801	3.6281	559.56962	3.2142	580.40375	3.6571
496.65493	3.5746	559.38116	3.6711	559.57277	3.1648	581.36004	3.6694
496.65876	3.5918	559.38431	3.7236	559.57591	3.1772	581.36249	3.6754
496.66261	3.5362	559.38746	3.6732	559.57904	3.3032	581.36494	3.7046
521.51586	3.5611	559.39066	3.6912	572.44511	3.3772	581.36741	3.7042
521.52041	3.5552	559.39468	3.7852	572.44758	3.5286	581.36985	3.6751
521.52497	3.5851	559.39783	3.7586	572.45008	3.5466	581.37231	3.6832
521.52953	3.6104	559.40099	3.6746	572.45256	3.5992	581.37476	3.7244
521.53425	3.6124	559.40414	3.6541	572.45503	3.6046	581.77211	3.7031
521.53881	3.6162	559.40728	3.5948	572.45751	3.5818	581.79721	3.6686
521.54336	3.5994	559.41043	3.5111	572.46111	3.5254	581.38224	3.6482
521.54791	3.5954	559.41357	3.5121	572.46247	3.5492	581.38469	3.6131
521.55246	3.5462	559.41672	3.5321	572.46495	3.5386	581.38721	3.4831
521.55701	3.5088	559.41988	3.5324	572.46743	3.4892	581.38966	3.4418
521.56174	3.4746	559.42302	3.5532	572.47054	3.5432	581.39211	3.4324
521.56631	3.4811	559.42635	3.5806	572.47303	3.5844	581.39456	3.4222
521.57085	3.4782	559.42948	3.5642	572.47551	3.6058	581.39702	3.3964
521.57541	3.4824	559.43262	3.5882	572.47798	3.6612	582.36147	3.4818
521.57996	3.5392	559.43577	3.6318	572.48046	3.6854	582.36464	3.5002
521.58451	3.5704	559.43893	3.6248	572.48294	3.6422	582.36781	3.4828
521.58923	3.5918	559.44208	3.6624	572.48541	3.6331	582.37098	3.4796
539.43564	3.6754	559.44522	3.7211	572.48791	3.6468	582.37415	3.5642
539.43948	3.6604	559.44837	3.6632	572.49038	3.6034	582.37731	3.5596
539.44332	3.6516	559.45152	3.5821	572.49286	3.5958	582.38049	3.4544
539.44717	3.6474	559.47861	3.5492	572.49941	3.5806	582.38365	3.4834
539.45101	3.6128	559.48175	3.4642	572.50436	3.5481	582.38682	3.5174
539.45485	3.5192	559.48489	3.4056	572.50931	3.5551	582.38999	3.4796
539.45869	3.5542	559.48802	3.4194	572.51185	3.5568	582.39321	3.4682
539.46254	3.5608	559.49116	3.5286	572.51433	3.5328	582.39638	3.5906
539.46644	3.5752	559.49431	3.5296	580.36381	3.5828	-----	-----
539.47028	3.5756	559.49743	3.5676	580.36631	3.5621	-----	-----